

NOTICE

PORTIONS OF THIS REPORT ARE UNCLASSIFIED. It has been reproduced from the best available copy to permit the broadest possible availability.

**UCRL-90494
PREPRINT**

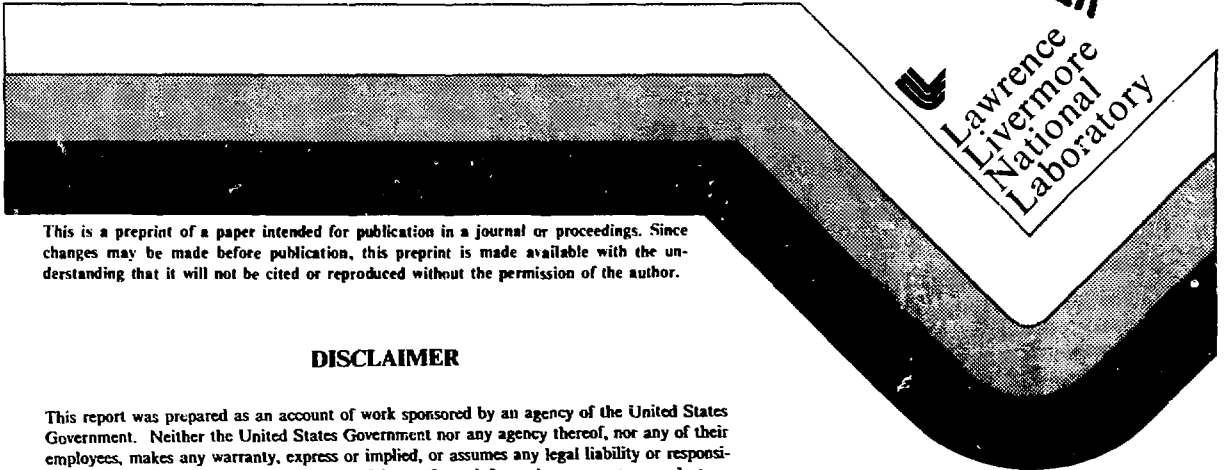
CONF-84-0887--2

Developments of Optical Fast-Gated Imaging Systems

H. A. Koehler and D. E. Kotecki

This paper was prepared for the Proceedings
of the 16th International Congress on
High Speed Photography and Photonics
Strasbourg, France
August 27-31, 1984

August 1984



This is a preprint of a paper intended for publication in a journal or proceedings. Since changes may be made before publication, this preprint is made available with the understanding that it will not be cited or reproduced without the permission of the author.

DISCLAIMER

This report was prepared as an account of work sponsored by an agency of the United States Government. Neither the United States Government nor any agency thereof, nor any of their employees, makes any warranty, express or implied, or assumes any legal liability or responsibility for the accuracy, completeness, or usefulness of any information, apparatus, product, or process disclosed, or represents that its use would not infringe privately owned rights. Reference herein to any specific commercial product, process, or service by trade name, trademark, manufacturer, or otherwise does not necessarily constitute or imply its endorsement, recommendation, or favoring by the United States Government or any agency thereof. The views and opinions of authors expressed herein do not necessarily state or reflect those of the United States Government or any agency thereof.

DISTRIBUTION OF THIS DOCUMENT IS UNLIMITED

Handwritten signature or initials

Developments of optical fast-gated imaging systems

H. A. Koehler and D. Koteck.

Lawrence Livermore National Laboratory, University of California
P.O. Box 808, Livermore, California 94550

Abstract

Several fast-gated imaging systems to measure ultra-fast single-transient data have been developed for time-resolved imaging of pulsed radiation sources. These systems were designed to achieve image recording times of 1-3 ms and dynamic ranges of >200:1 to produce large two-dimensional images ($\geq 10^4$ spatial points) of 1-2 ns exposure and small two-dimensional images (≥ 200 spatial points) of ≤ 0.5 ns exposure. Both MCP intensified solid-state two-dimensional framing cameras and streak camera/solid-state camera systems were used; the framing camera system provides snap shots with high spatial resolution whereas the streak camera system provides for limited spatial point, each with high temporal resolution. Applications of these systems include electron-beam, x-ray, gamma-ray, and neutron diagnostics. This report reviews the characteristics of the major components of fast-gated imaging systems developed at Lawrence Livermore National Laboratory. System performances are described in view of major experiments, and the diagnostic requirements of new experiments in atomic physics (x-ray lasers) and nuclear physics (fusion) are indicated.

Introduction

Several fast-gated imaging systems have been investigated to measure ultra-fast single-transient data from pulsed radiation sources. Work on these systems was stimulated by increased demand at Lawrence Livermore National Laboratory (LLNL) for diagnostic systems of this type. These systems were designed to achieve the following criteria:

- Image recording time into memory of 1-3 ms and
- Broad sensitivity/dynamic range of >200:1

to produce:

- Large two-dimensional images ($\geq 10^4$ spatial points) of 1-2 ns exposure and
- Small two-dimensional images (≥ 200 spatial points) of ≤ 0.5 ns exposure.

Generally, these imaging systems are sophisticated pinhole cameras using a pinhole or slit to focus x rays, gamma rays, or neutrons onto a converter (fluor); visible light from the fluor is focused onto the photosensors of the recording camera. Fast shuttering of these images is provided by both gated microchannel-plate (MCP) intensifiers and streak cameras that are placed on front of the recording cameras. The recorded images are digitized and stored in nonvolatile memories. Physically meaningful pictures are obtained after computer processing of the experimental and calibration data.

Applications of these systems include electron-beam, x-ray, gamma-ray, and neutron diagnostics. Electron-beam diagnostics are used to provide information about the size and position of the beam, currents in the beam, and its propagation characteristics. X-ray diagnostics are used to make time-resolved x-ray measurements. Gamma-ray and neutron diagnostics include electronic pinhole neutron experiments and tomography, which are used to study burn efficiencies and implosion symmetries of fission/fusion devices.

This report reviews the characteristics of the major components of fast-gated imaging systems that have been developed in the Nuclear Test Program of LLNL. The system performances are described in view of major experiments.

Imaging system components

The major components of a gated imaging system are the shutter, the camera, and the data acquisition system. The shutter may be a MCP intensifier, a streak camera, or an internal gating grid. The camera may be either a solid-state Reticon using 100×100 , 256×256 , or 1024×1 photodiode array sensors, a Fairchild camera using 488×380 charge-coupled device (CCD), or a vacuum-tube General Electric FPS-GSIT (focus-projection-scan: gated silicon intensified target) vidicon camera. The digital data acquisition systems used for all cameras consist of memories, computers, and recorders.

Optical shutters

Gated MCP intensifiers and streak cameras have been examined extensively as optical shutters of fast-framing cameras.^{1,4}

MCP intensifiers. The MCP intensifier consists of a photocathode (PC), a MCP electron multiplier, and a phosphor screen that constitutes the photon source viewed by the camera. The photocathode is proximity focused (~ 0.25 mm) onto the MCP ($\sim 10^5$ electron gain), which is in turn proximity focused (~ 1.25 mm) onto the phosphor screen. Optical shuttering is achieved by applying a voltage pulse between the PC and MCP or across the MCP. The MCP intensifier is gated by dc reverse-biasing and by pulse forward-biasing. Both coaxial termination geometry and microstrip transmission-line geometry are used.^{1,4}

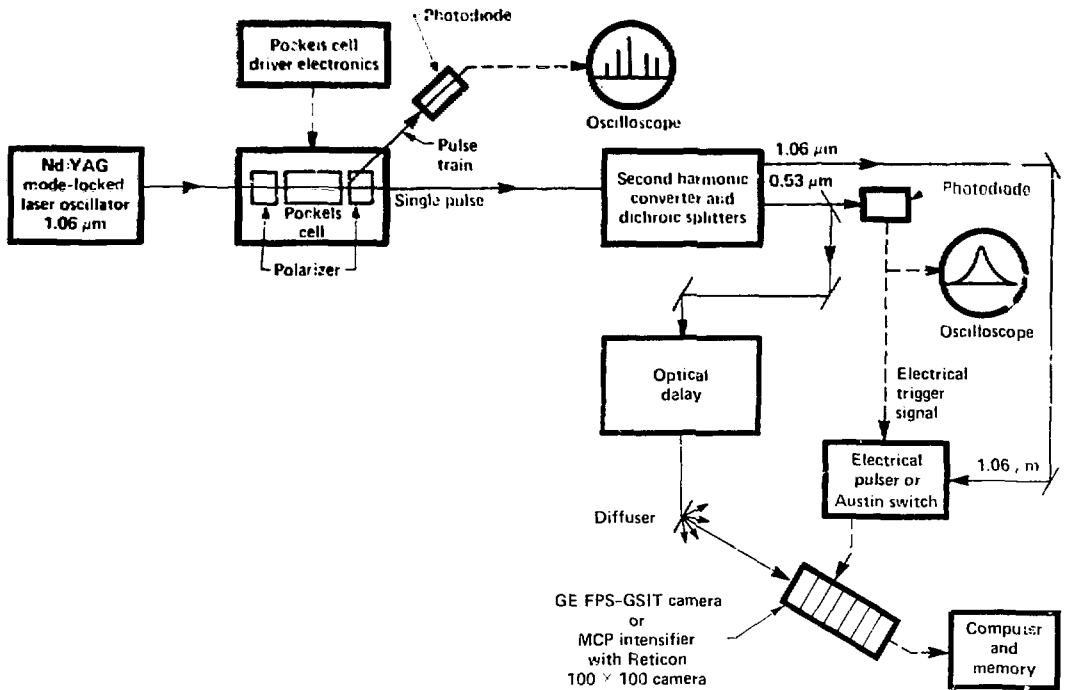


Figure 1. Calibration arrangement for correlating optical shutter speed to spatial resolution.

For most high-speed imaging applications, the correlation of optical shutter speed to spatial resolution at a fixed contrast transfer function (CTF) must be precisely determined. Figure 1 shows a typical calibration arrangement. A single pulse from a mode-locked Nd:YAG laser ($1.06 \mu\text{m}$ and 29 ps FWHM) produces an electrical gate pulse (by providing a trigger from a photodiode for an avalanche transistor pulser or by energizing a photoconductive switch). A portion of the original pulse is frequency-doubled at 532 nm ; this pulse travels through an optical delay line of $40\text{-}140 \text{ ns}$ (adjustable in 50-ps steps) onto a diffuser. A MCP intensifier coupled to a Reticon 100×100 photodiode array or a FPS-GSIT is placed behind the diffuser, at 45° with respect to the beam axis. The optical shutter length is measured by increasing the optical delay of the frequency-doubled laser pulse in relation to the fixed electrical gating pulse. The digital output of the camera is sent to a minicomputer and recorded on a floppy disk for image processing.

Figure 2 shows the relation of uniformity vs time for a typical gated 18-mm MCP intensifier. The iris effect (shading) is caused by the electrical surface resistance of the photocathode undercoating. Reduced photocathode resistance ($< 10^2 \Omega/\text{square}$) is essential for fast gating.

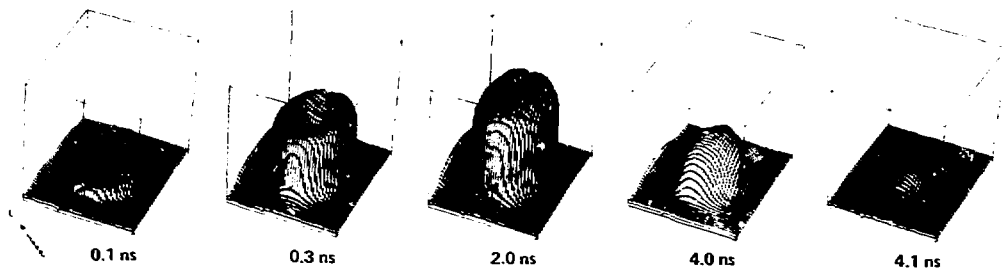


Figure 2. Uniformity vs time for a typical gated 18-mm MCP intensifier. The iris effect (shading) is caused by the electrical surface resistance of the photocathode undercoating.

Table 1 summarizes the performance characteristics of the MCP intensifier that was used as an optical shutter at 570 nm. Currently, standard 14111 ITT 18-mm-diameter MCP intensifiers (with a chromium substrate PC) provide a gating speed of 1.90 ns at 2 line pairs/mm and 70% CTF. We are continuing our efforts to increase the optical shutter speed of MCP intensifiers. Preliminary results of gating MCP intensifiers having GaAs photocathodes showed that optical shutters of 1 ns can be obtained in a microstrip transmission-line geometry. Experiments with sector gating, segmented PCs, and with triple-thickness PCs at Los Alamos National Laboratory (Los Alamos, NM) increased the gating speed to 1.5 ns.^{5,6}

Table 1. Performance characteristics of the MCP intensifier and the streak camera.

Characteristic	Goal	MCP intensifier ^a	Streak camera ^b
Shutter speed (ns)	$\ll 1.0$	1.9 (< 1.0) ^c	0.05-500 ^d
Resolution (lp/mm) ^f	8	2	4
Resolvable points	100,000	10,000 ^f	250
Extinction ratio	10 ⁶ :1	$> 10^6$:1	10 ⁶ :1
Dynamic range	> 200 :1	200:1 ^g	100:1
Gain (radiometric)	10 ⁴	10 ⁴ (10 ³) ^f	500
Temporal samples	> 1	1	380 ^h
Saturation (erg/cm ²) at 570 nm	—	10 ⁻³	10 ⁸ -10 ⁴ /s ⁱ

^a 18-mm diameter.

^b With 40-mm-diameter MCP intensifier.

^c GaAs photocathode.

^d 0.5% of sweep time, where sweep time is 0.01-100 μ s.

^e At 70% CTF.

^f With Reticon 100 \times 100 camera.

^g Using 8-bit digitizer.

^h Fairchild 244 \times 380 CCD.

ⁱ Corresponding to a sweep time of 0.01-100 μ s.

We are currently designing a portable electrical pulser that produces > 300 V with a pulse width of < 0.5 ns (with < 0.1 ns jitter) into an impedance load of 17 Ω .⁷⁻⁹ Specially packaged step recovery diodes and photoconductive switches driven by laser diodes are considered in these designs.^{4,5}

Streak cameras. Streak cameras are optical shutters; they convert a pulse of light from a point source into a streak whose points correspond to the temporal sequence of the light intensity. Light strikes the photocathode through a slit and generates a pulse of photoelectrons that is accelerated toward a phosphor screen. The electrons are deflected by sweep electrodes and spread out on the phosphor screen. Generally, the screen is viewed by a camera through a MCP intensifier.

The streak camera described in this report was built around the RCA 73435 AK and AJ series tube.¹ This tube is a gated electrostatic-focus, electrostatic-deflection image device that is specifically designed for high-speed light shutters. The image tube has a fiber-optic or glass input window and a fiber-optic output window, a modified S-20 photocathode (allowing extended UV and IR response), and a P-11 phosphor. This tube was chosen because of its relatively large PC (60 \times 25 mm), which permits 250 resolvable lines at 70% CTF. Single photoelectrons can be observed at the phosphor. The extraction grid is pulse-biased to improve the extinction ratio (to $\sim 10^6$). A 40-mm-diameter ITT MCP intensifier having an S-20 PC and a P-20 phosphor coupled to the streak tube by fiber optics provides a sensitivity adjustment as well as a better spectral match to the silicon response of the solid-state recording cameras. Adding a MCP intensifier to the streak camera, however, degrades the spectral resolution. For instance, at 70% CTF and 150 ns sweep, the spatial resolution with and without the MCP intensifier is 4 and 5.5 lp/mm, respectively. Table 1 summarizes the streak-camera performance.

We are currently investigating the feasibility of replacing the RCA streak tube with one of increased quantum efficiency at 820 nm and larger spatial resolution. Development work is currently being conducted by both ITT Electro-Optics Products Division (Fort Wayne, IN) and EG&G, Inc. (San Ramon, CA) to meet these higher performance goals.

Cameras

We have examined three kinds of cameras: solid-state Reticon and Fairchild cameras, and vacuum-tube GE FPS-GSIT vidicon cameras.

We used a modified TV Optoliner (Optical Instruments Corp.) and a pulsed light source to measure the linearity to incident light, dynamic range, spatial uniformity, and absolute sensitivity for each camera at a fixed wavelength. The output energy of the Optoliner was measured using a calibrated photodiode. Calibrations of the cameras were performed by averaging the output of all pixels for each Optoliner pulse taken at different intensity levels.

Reticon cameras. The main components of the Reticon solid-state camera system are the camera controller, the camera head (containing the sensor and preamplifier), and the power supply. The controller contains the amplifier, digitizer, and clocks.

The two-dimensional-array Reticon cameras described in this report use monolithic silicon chips that contain a 100×100 or 256×256 photodiode matrix as well as access switches and MOS shift registers for scanning in the x and y directions. The x and y shift registers access each photosite, and the charge held in each photosite is serially transferred onto a video line common to all photosites.^{4,10} More specifically, the signal transport mechanism of the Reticon 100×100 uses one y -shift register to select rows and two x -shift registers to select individual photosites in each row. Charges are transferred in parallel into two registers (bucket-brigade shift registers)—one for the even columns and one for the odd columns. The photosites are reset in each row, and the odd and even column charges are clocked to serial output.

Reticon 100×100 . We measured the linearity, dynamic range, resolution, and saturation of this camera (Table 2). The array size is 6×6 mm, the center-to-center spacing of the photosites is $60 \mu\text{m}$, and the active area is 58% of the array size.

The camera was designed at LLNL. Variations from commercially available cameras included decreasing the read-out rate to 2.5 ms/frame, digitizing the video output signal, and repackaging the camera for operating in an adverse environment. The cameras were designed to be reset on receiving a trigger signal, thus allowing them to record pulsed light images. Also, the absence of automatic gain control enabled the camera to be used as a diagnostic of absolute energy measurements. The Reticon 100×100 array can be outfitted with a fiber-optic faceplate to allow for fiber-optic coupling of a MCP intensifier tube.

Reticon 256×256 . We are also presently testing a new camera that provides larger spatial resolution.¹¹ This camera uses a Reticon 256×256 photodiode array sensor. The array size is 10.24×10.24 mm, the center-to-center spacing of the photosites is $40 \mu\text{m}$, and the active area is 63% of the array size. Table 2 summarizes the performance goals. Saturation sensitivity of $\sim 1.5 \text{ erg/cm}^2$ at 570 nm is desired since most solid-state cameras are coupled to MCP intensifiers that have a maximum output of $\sim 1.2 \text{ erg/cm}^2$.

The architecture of the array consists of eight contiguous blocks of 32×256 photosites, each having its own 5 megapixel video output. With additional multiplexing of two video lines each, a frame time of 1.6 ms is expected.

Reticon 1024×1 . A Reticon 1024×1 linear array of silicon photodiodes is used with spectrometers in high-speed diagnostic systems. The array size is $12.5 \mu\text{m} \times 2.5$ mm, the center-to-center spacing of the photosites is $25 \mu\text{m}$, and the active area is 50% of the array size. Table 2 summarizes the characteristics of this camera.¹²

Fairchild camera. The solid-state Fairchild camera described here was designed at LLNL.^{13,14} It uses 380 horizontal and 488 vertical charge-coupled photoelements. The dimensions of the array are 8.8 mm horizontally and 11.4 mm vertically. Center-to-center spacings are 30 and $18 \mu\text{m}$ in the horizontal and vertical directions, respectively. The active area is 40% of the array size.

Photoelectrons collected in the photosites are transferred first from the odd-numbered rows to a vertical transport register, then to a horizontal transport register. The even-numbered photosite rows are read-out next in a similar manner. To adapt this camera to a high-speed diagnostic system, every two consecutive rows are combined (on-chip addition, OCA) and the clocking rate of the array is increased. The analog video output is digitized at 20 MHz (8 bits). This noninterlaced, one field/frame format provides a frame time of 5 ms. Table 2 lists some of the characteristics of this camera. The dynamic range of the camera is limited by the 8-bit digitizer to 256:1. Adjusting the camera gain for increased sensitivity decreases the dynamic range. Contrary to the Reticon photodiode arrays, the CCD sensors exhibit "blooming" at $\sim 3 \times$ saturation value in the vertical direction only.

Figure 3 shows a typical response of a gated 2.6-ns MCP intensified Fairchild 244×380 camera to a uniform optical field of varying intensity from the Optoliner. (Figure 3 indicates three typical flat-field responses.) A least-squares fit was performed on the discrete data points. The camera saturated at 1.2 merg/cm^2 using 570-nm light. The standard deviation of the recorded output from all photosites is shown as vertical bars; 30 counts out of 223 counts was the worst case. This includes the shading inherent in the pulsed light source. The total operating range of 220 counts is determined by the background (lower limit) and the digitizer (upper limit). Generally, fixed-pattern noise and random fluctuations are less than 0.5% of the saturation level.

Table 2. Performance characteristics of Reticon cameras and the Fairchild CCD.

Characteristic	Goal	Reticon photodiode array			Fairchild CCD
		100×100	256×256	1024×1	244×380
Pixels	10^5	8	12 ^b	7	6×8
Resolution (lp/mm) ^a	15	8	12 ^b	7	6×8
Frame time (ms)	<2	2.5	1.8 ^b	1	5
Dynamic range ^c	>200:1	500:1	500:1 ^b	1000:1	750:1
Saturation (erg/cm^2) ^d	<1.5 ^b	1.7 (0.002) ^e	1.5 ^b	0.8	0.9 (0.001) ^e
Digitizer (bit)	10	8	9 ^b	10	8
Field uniformity (%) ^d	±30	>95	>95 ^b	>95	>95

^a At 70% CTF.

^b Design goals.

^c Photosensor only; dynamic range is maximum signal/RMS noise.

^d At 570 nm.

^e With MCP intensifier (fiber-optic input).

Table 3. Performance characteristics of the GE FPS-GSIT vidicon camera.

Characteristic	GE FPS-GSIT vidicon camera ^a
Pixels	470×256^b
Resolution (lp/mm) ^c	5
Frame time (ms)	≥1.6
Dynamic range ^d	≥(50-200):1
Saturation (erg/cm^2) ^e	0.01
Digitizer (bit)	8
Field uniformity (%)	≤75
Gating speed (ns)	≥0.5
Extinction ratio	(60-1000):1

^a 25-mm-diameter S-20 photocathode.

^b 3.2-ms read-out.

^c At 70% CTF with 1 to 2-ns gate.

^d Photosensor only.

^e At 570 nm.

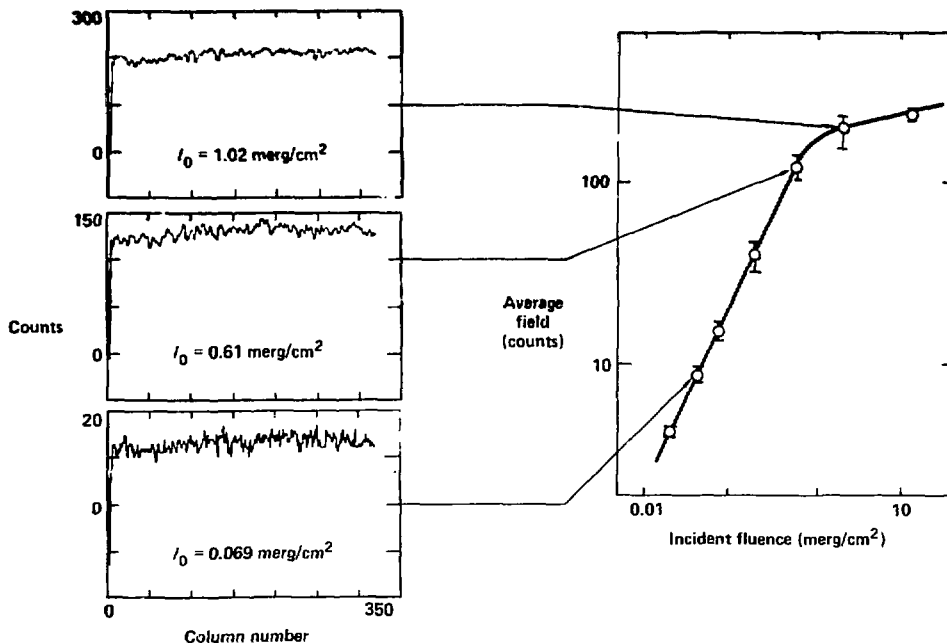


Figure 3. Response of a gated MCP intensified Fairchild 244×380 camera to a uniform optical field of varying intensity. The optical gate was 2.6 ns and the calibration wavelength was 570 nm. Three typical flat-field responses are shown.

GE FPS-GSIT vidicon camera. The GE FPS-GSIT vidicon camera consists of a camera head and a control unit. This camera is the result of extensive development at Los Alamos National Laboratory.^{5,6} The camera head contains the image sensor, amplifiers, biasing and deflection circuits. The controller contains power supplies, video processing and shading correction circuitry. The camera was designed to reset to the beginning of the field upon receiving a trigger signal. The deflection circuits are reactivated after an adjustable delay during which the cathode is blanked. The time delay is used to integrate the pulse image on the sensor so that the entire pulse is received before read-out of the sensor begins. The image format is 256 scan lines/field, noninterlaced. The read-out can be varied from 1.6 to 25.6 ms. A 40-MHz digitizer and a 1.6-ms frame time provides an image size of 236 columns by 256 rows. For a 3.2-ms frame time, the number of columns is increased to 472.

The FPS-GSIT can be gated to produce optical shutters with durations as short as 500 ps. Photoelectrons from the S-20 photocathode pass through the gating grid and are electrostatically focused onto the other side of the silicon target. The video output signal is proportional to the beam current necessary to recharge the silicon target diodes to the cathode potential.

The optical shutter speed of the FPS-GSIT vidicon was recently measured using the RF LINAC at the EG&G facility in Santa Barbara, CA. A Faraday cup in the LINAC beam produced a 200-ps FWHM gating pulse that resulted in an optical shutter of ~500 ps FWHM. Because the photocathode was coated after installation into the tube envelope near the gating grid, the measured extinction ratio was only ~60:1. (The extinction ratio is defined as the ratio of light intensities that, when focused onto the PC when the tube is gated off and on, produce the same output signal.) Table 3 summarizes the performance characteristics of the FPS-GSIT vidicon camera.

Comparison of cameras. The Reticon 100×100 photodiode array and the Fairchild 244×380 CCD solid-state cameras have been used extensively at LLNL for high-speed imaging. The Reticon 1024×1 linear array has been used only recently with spectrometers. The Reticon 256×256 is still under development. Some applications of these cameras are discussed below.

The advantages of the MCP intensified solid-state cameras over vacuum-tube FPS-GSIT vidicon cameras are excellent field uniformity and linearity, small geometric distortion, relatively large linear dynamic range, a large extinction ratio, and compactness. The disadvantages are relatively slow optical gating speed and low spatial resolution.

The advantages of the vacuum-tube FPS-GSIT camera over the MCP intensified solid-state cameras are fast gating speed and a large photocathode, which provides excellent spatial resolution. Disadvantages are low linear dynamic range, poor field uniformity, shading, geometric distortion, low shutter ratio, and larger size. Work is in progress at Los Alamos National Laboratory to improve

the shutter ratio and the linear dynamic range. The FPS-GSIT camera has not yet been incorporated into a high-speed diagnostic system at LLNL.

Data acquisition system

The Reticon 100×100 photodiode array cameras use a data acquisition system designed at LLNL (Fig. 4). The bit/frame synchronizing module deserializes the 45-Mbit/s serial Bi-M PCM data stream from the 100×100 Reticon camera. The memory is a dual-port, 16K, 9-bit static RAM. The unit memory controller (UMC) is a minicomputer (LSI 11/23) that controls the data transfer to permanent storage. Local processing of the data with the minicomputer includes background subtraction, intensity profiles, histograms, contour plots, and three-dimensional isometric plots.

The Reticon 256×256 and 1024×1 photodiode-array camera and the Fairchild 380×488 CCD camera use similar data acquisition systems (Fig. 4). A real-time image processor (Recognition Concept Inc.) is used in conjunction with a minicomputer to transfer data to the nonvolatile memories and to permanent storage. This minicomputer performs the same image processing functions available for the Reticon 100×100 , with the addition of pseudo-color enhancement and image magnification.

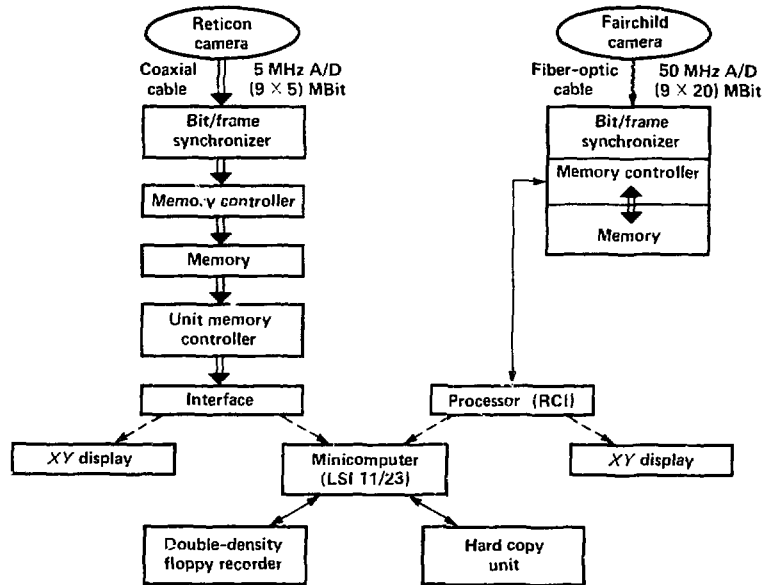


Figure 4. Data acquisition systems used by the Reticon photodiode array and Fairchild CCD cameras.

Imaging system applications

High-speed optical imaging systems are used in the Nuclear Test Program at LLNL with pulsed radiation sources in the laboratory and in the field, on accelerators, lasers, and nuclear tests. In general, MCP-gated solid-state framing cameras provide one snapshot of an event with high spatial resolution whereas streak camera/solid-state camera system provide high temporally resolved images with limited spatial resolution.

Applications using MCP and solid-state cameras

The Reticon and Fairchild solid-state cameras are coupled to a MCP intensifier (18, 25, or 40 mm in diameter) with a fiber-optic reducer. The coupling and interfaces greatly affect the gain and spatial resolution of the camera system. For instance, the spatial resolution for a camera with and without a MCP intensifier differs by as much as 40%. Also, an increase in MCP intensifier gain reduces the dynamic range and saturation value of the camera system (i.e., decreases the slope of the linearity curve, Fig. 3). For this reason, all cameras are calibrated with and without a MCP intensifier to assure proper coupling between the components.

Electron-beam diagnostics. Relativistic electron-beam cross sections and beam currents are measured by focusing Cerenkov radiation from thin plastic foils onto fiber-optic arrays that are coupled to gated MCP intensifiers. Cerenkov foils are used as beam current monitors if the plasma current contributes significantly to the air fluorescence.

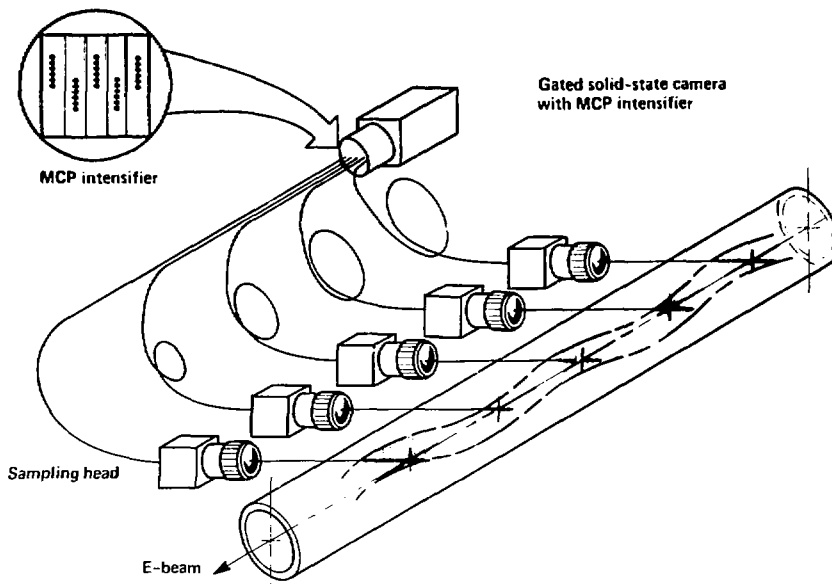


Figure 5. Experimental configuration for observing electron-beam propagation instabilities in a drift tube.

To observe electron-beam propagation instabilities in a drift tube, the air fluorescence is focused onto fiber-optic arrays that are placed along the drift-tube axis (Fig. 5). To assure equal arrival time of the optical signals at the gated MCP intensifier, the fiber-optic arrays are cut at different lengths commensurate with the transit time of the photons through the fiber-optic bundles and with the time-of-flight of the electrons between the sampling heads.

The size and position of a relativistic electron beam inside a wiggler magnetic field of a free-electron laser is determined using a tantalum/fluor arrangement in the waveguide.¹⁵ One end of a fiber-optic bundle is connected to this fluor and the other end to a gated MCP intensifier that is coupled to a Reticon 100 × 100 photodiode array camera. This camera is located outside the accelerator shield wall.

X-ray diagnostics. Time-resolved x-ray measurements are performed with a Reticon linear photodiode array camera. Efforts are made to use 7 to 28 linear arrays with 1 to 4 MCP detectors in a microstrip transmission-line geometry to observe x rays of several keV from a bent-crystal spectrometer¹⁶ with resolution of a few eV. Jacoby³ has shown that, compared to termination coupling, MCP intensifiers having a microstrip transmission-line geometry permit high-speed optical shuttling. The MCP detector shown in Fig. 6 was designed by Eckert.¹⁶ This detector uses seven gold microstrip lines on the input side (x-ray side) of the MCP. An electrical 1-kV pulse applied across the MCP results in a 0.5-ns FWHM optical gate. Electrons from the MCP are accelerated by a 3-kV, 10- μ s electrical pulse onto a P-46 phosphor deposited on a fiber-optic face plate (proximity-focused diode). To separate the camera from the high-radiation environment near the MCP detector and to increase the signal-to-noise ratio, fiber-optic arrays couple the P-46 output corresponding to each strip line onto a gated (5 kV, 150 ns) proximity-focused diode. Coherent fiber-optic bundles then transfer the images to seven Reticon linear arrays. The arrays are read-out in 1 ms at 180 Mbit/s.

Gamma-ray and neutron diagnostics. An electronic pinhole neutron experiment uses a gated MCP intensified Reticon or Fairchild solid-state camera to study burn efficiencies and implosion symmetries of fission/fusion devices. In the experiment, nuclear radiation is focused through a pinhole onto a plastic fluor.¹ Light from the fluor is then focused onto the camera that digitizes the data and sends them to a memory. These data and the calibration data are processed by computer into a quantized image.

Applications using streak cameras and solid-state cameras

A Fairchild CCD camera coupled to a MCP intensified streak camera is used for tomography and for time-resolved studies of electron-beam propagation phenomena and nuclear fusion processes. Table 4 lists the performance characteristics for this system.

Electron-beam diagnostics. Time-resolved one-dimensional images of a 30-ns electron beam were obtained.¹⁷ A lens focused the air fluorescence produced by the beam-air interaction onto three fiber-optic arrays positioned around the beam axis. The fiber-optic arrays are connected to a streak camera positioned behind an accelerator shield wall. Two-dimensional images were reconstructed from the data using the maximum-entropy tomographic technique. These images were combined to produce a high-speed movie of the electron-beam pulse propagation in air.

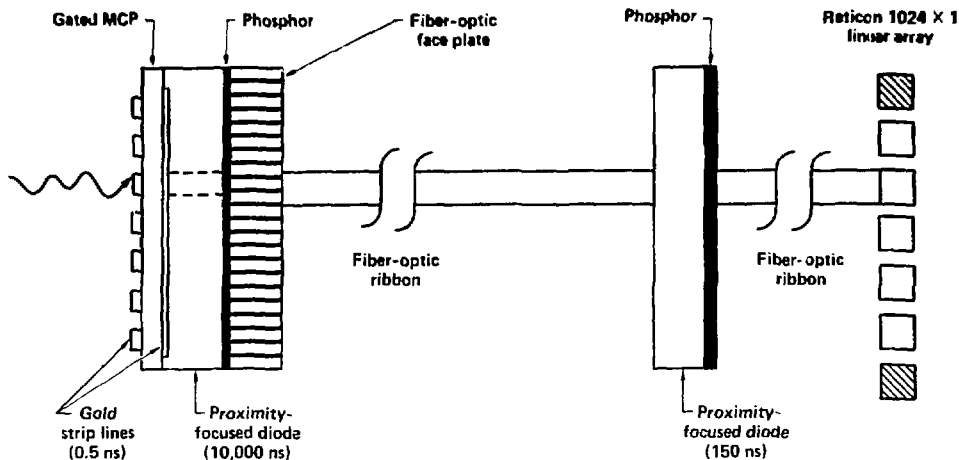


Figure 6. Experimental configuration for measuring time-resolved x-ray spectra.

Table 4. Performance characteristics of MCP intensified streak camera/Fairchild CCD system.

Characteristic	MCP ^a intensified streak camera/ Fairchild CCD system ^b
Shutter speed (ns)	0.05-500 ^c
Resolution (lp/mm) ^d	4
Frame time (ms)	4.9
Dynamic range	100:1
System gain	20
Saturation (erg/cm ² ·s) at 570 nm	10 ⁸ -10 ⁴
Digitizer (Mbit/s)	180 ^e
Sensitivity (photoelectron/pixel)	1 ^f

^a 40-mm-diameter, supplied by ITT.

^b 244 × 380 pixels.

^c 0.5% of sweep time, where sweep time is 0.01-100 μs.

^d At 70% CTF, 250 lines total.

^e 8 bits, parity, overhead.

^f At streak camera phosphor.

Nose-erosion studies of high-current relativistic electron beams have been performed with a system similar to that used for determining electron-beam propagation instabilities. To obtain nanosecond rise-time information, the MCP was replaced by a streak camera.

Neutron diagnostics. A tomographic system with four slits is used to provide two-dimensional time-resolved images of fusion devices.¹⁸ A pinhole images the ionizing radiation onto the floor, and the four slits image sections of the floor onto four fiber-optic arrays. This system uses a Fairchild CCD and streak camera and a wide-bandwidth fiber-optic transmission system to transfer the data into the memory.

The streak camera/solid-state camera system is also used for measuring the spatial dependence of temperature in fusion cavities. Essentially, this experiment is similar to the four-slit tomographic arrangement except that the slits are replaced by a lens.

Conclusions

Time-resolved imaging is an important diagnostic of pulsed radiation sources at LLNL—in the laboratory as well as in the field. Both the MCP intensified solid-state two-dimensional framing cameras and the streak camera/solid-state camera system are complementary.

The framing camera provides for snap shots with high spatial resolution. In general, these cameras are capable of 10⁵ spatial points, 2-ns optical gate time, 2-ms frame time, and 200:1 dynamic range.

The streak camera system provides for limited spatial points each with high temporal resolution. These systems are generally characterized by 250 spatial points, 0.05-ns temporal resolution, 5-ns frame time, and 100:1 dynamic range.

New cameras are being developed to meet the demand for higher temporal and spatial resolution, faster frame time, larger dynamic range, and better data processing and data archiving systems. Fast diagnostic systems that use the Reticon 256×256 and 1024×1 photodiode arrays have been developed and incorporated into experiments. Work continues on studying low-resistivity photocathode and low-impedance high-voltage pulsers for fast gateable MCP.

References

1. Lear, R., "Fast Imaging Applications in the Nuclear Test Program," in IEEE Trans. Nuclear Science, Feb. 1984, Vol. NS-31 (1), pp. 495-503.
2. Koehler, H. A., and Cornish, J. P., MCP intensifier characterization Lawrence Livermore National Laboratory, Livermore, CA, ATA Note 192, private communication (Jan. 11, 1983).
3. Jacoby, B. A., Kotecki, D. E., and Lear, R. D., "Direct Gating of Microchannel Plates," IEEE Trans. Nucl. Sci., Vol. NS-30 (6), pp. 4624-4627, Dec. 1983.
4. Kotecki, D. E., and Lear, R., "Optical shutters using microchannel plate (MCP) intensifier tubes," in Proc. Soc. Photo-Optical Instrumentation Engineers, 1983, San Diego, CA, Aug. 1983 (SPIE, Bellingham, WA), Vol. 427, pp. 62-78, 1983.
5. Yates, G. L., King, N. S. P., Jaramillo, S. A., Noel, B. W., Globy, P. L., Aeby, I., and Detch, J. L., "Nanosecond Image Shuttering Studies at Los Alamos National Laboratory," in IEEE Trans. Nuclear Science, Feb. 1984, Vol. NS-31, pp. 484-489.
6. Yates, G. L., King, N. S. P., Jaramillo, S. A., Ogle, J. W., and Noel, B. W., "Image shutters: gated proximity focused microchannel plate (MCP) wafer tubes versus gated silicon intensifier target (SIT) vidicons," in Proc. 15th International Congress on High-Speed Photography and Photonics, 1982 (SPIE, Bellingham, WA), Vol. 348, pp. 422-433, 1982.
7. Yates, G. L., Ogle, J. W., and King, N. S. P., "Overview of pulses for nanosecond gating of image shutter tubes," in Proc. 15th International Congress on High-Speed Photography and Photonics, 1982 (SPIE, Bellingham, WA), Vol. 348, pp. 434-437, 1982.
8. Li, K. K., Whinnery, J. R., and Dienes, A., "Optical switches for generation and pulse shaping of ultrashort electrical pulses," Picosecond Lasers and Applications, 1982 (SPIE, Bellingham, WA), Vol. 322, pp. 124-130, 1982.
9. Lee, C. H., "Picosecond Optoelectronic Switching in GaAs," Appl. Phys. Lett., Vol. 30 (2), pp. 84-86, 1977.
10. Sammons, T. J., EL PINEX Handbook, EG&G/SRO, San Ramon, CA, EGG1183-4229 (Jan. 1982).
11. Tseng, H., and Lin, C., "A High Frame Rate RA 256×256 Solid State Image Sensor," Electronic Imaging '84, Boston, MA, Sept. 11-13, 1984 (Society of Photographic Scientists and Engineers, Springfield, VA).
12. O'Brien, C. R., Lawrence Livermore National Laboratory, Livermore, CA, private communication (1984).
13. Koehler, H. A., and Clendener, L., Fairchild CCD-2000 camera characterization, Lawrence Livermore National Laboratory, Livermore, CA, ATA Note 196, private communication (Jan. 13, 1983).
14. Stephenson, P. S., Lawrence Livermore National Laboratory, Livermore, CA, private communication (1984).
15. Orzechowski, T. J., Koehler, H. A., and Edwards, W., "A novel probe for determining the size and position of a relativistic electron beam," in Proc. Soc. Photo-Optical Instrumentation Engineers, San Diego, CA, Aug. 19-24, 1984 (SPIE, Bellingham, WA).
16. Eckert, M., and O'Brien, C. R., Lawrence Livermore National Laboratory, Livermore, CA, private communication (1984).
17. Koehler, H. A., Jacoby, B. A., and Nelson, M., "Time-resolved tomographic images of a relativistic electron beam," in Proc. Soc. Photo-Optical Instrumentation Engineers, San Diego, CA, Aug. 19-24, 1984 (SPIE, Bellingham, WA).
18. Jacoby, B. A., Lawrence Livermore National Laboratory, Livermore, CA, private communication (1984).

Acknowledgments

We thank the following people from LLNL for their contributions: Richard Lear, Barry Jacoby, Mark Eckert, Hal Schulte, Charles O'Brien, Paul Stephenson, and Lamar Oik. Mauro Fardo and Tim Sammons from EG&G/SRO also supplied information for this paper. This work was performed under the auspices of the U.S. Department of Energy by Lawrence Livermore National Laboratory under Contract W-7405-Eng-48.